

Far-infrared imaging antenna arrays

Dean P. Neikirk, David B. Rutledge, and Michael S. Muha

Division of Engineering and Applied Science, California Institute of Technology, Pasadena, California 91125

Hyeon Park and Chang-Xuan Yu

Department of Electrical Sciences and Engineering, University of California, Los Angeles, California 90024

(Received 21 September 1981; accepted for publication 17 November 1981)

A far-infrared imaging antenna array has been demonstrated for the first time. The array is a line of evaporated silver bow-tie antennas on a fused-quartz substrate with bismuth-microbolometer detectors. The measured optical transfer function shows that the system is diffraction limited. This imaging array should find direct application in fusion plasma diagnostics. If the microbolometers can be replaced by more sensitive diode detectors, the array should also find application in radiometry and radar.

PACS numbers: 42.80.Qy, 84.40.Jh, 07.62. + s, 85.40. — e

Most current far-infrared and millimeter imaging systems depend on a single detector with mechanically scanned optics.¹⁻³ For many applications, however, this approach is inadequate. The required integration time may be long, or events may happen too quickly. In plasma diagnostics, this problem has been attacked by using as many as eight separate detectors.⁴ Several researchers have pointed out that an imaging array would be an important advance, and that it would be most attractive in monolithic integrated-circuit form.⁵⁻⁸ This is particularly true in view of recent progress in developing new planar detectors: Schottky diodes,⁹ superconductor-insulator-superconductor (SIS) junctions,¹⁰ and microbolometers.¹¹ We report here a monolithic line array and optical system with diffraction-limited resolution.

Figure 1 shows the approach. A lens system focuses an image through the substrate onto an antenna array. An image is obtained by plotting the signal received by each antenna. The system is similar to an oil-immersion microscope, except that the position of the object and the image are interchanged. This "reverse-microscope" design has several advantages. Spherical aberration and coma can be reduced to a low level.¹² Incident power is coupled efficiently into the antennas, because antennas on dielectric substrates are more sensitive to radiation coming from the substrate.¹³ In microwave tests on large-scale models, we found that 50% of the power focused by the objective lens is coupled into the array.¹³ We also found that cross-talk between neighboring antennas is low: 19 dB down for adjacent antennas.

The antenna array design is shown in Fig. 2(a). The antenna spacing is a compromise that gives adequate sampling, coupling efficiencies, and antenna patterns. The antenna is a modified bow tie. One unusual feature of this antenna is that the low-frequency leads are formed by extending the arms of the bow. No additional rf isolation is necessary. The bow angle of 60° gives an impedance of 150 Ω to match to the bismuth microbolometers. Reference 13 gives the design details. Figure 2(b) is a photomicrograph of one antenna. The substrate is fused quartz. The antennas are evaporated silver 75 nm thick with a spacing of 310 μm . The narrow lines are evaporated bismuth, also 75 nm thick. All patterns are formed by contact photolithography and lift-off. The dc resistances of the bolometers lay in the range

100–150 Ω .

The far-infrared measurements were made at 1.23 mm using a CO₂-pumped C₁₃ methyl-fluoride laser with a power output of 3 mW. The TPX objective lens had a 70-mm focal length and a 50-mm diameter. The fused-quartz substrate lens had a 6.62-mm radius. The thickness of the lens-substrate combination was 10 mm. To provide a point source, we focused the laser beam with another TPX lens to a spot a few millimeters in diameter at a distance of 1.4 m from the imaging system. When focused on this spot, the optical system had a magnification of 3.2° in the far field per millimeter in the image plane. This corresponds to 1.0° per antenna.

First we measured the system *E*-plane and *H*-plane patterns at a single antenna by rotating the imaging system. Both patterns are plotted in Fig. 3, along with the theoretical Airy pattern for the objective lens. The *E*-plane pattern has larger sidelobes than the Airy pattern. This probably results from the fact that the feed pattern of the bow-tie antenna on a substrate has a split in the *E* plane.¹³ We also measured the maximum response at each antenna. All subsequent measurements were normalized to these maxima.

Next, we determined the optical transfer function (OTF). With our array, we measure a discrete point-source response instead of the usual continuous response. This modifies the formula for the OTF.¹³ We found the point-source response by orienting to give a maximum at one antenna, and measuring the signals at neighboring antennas. This is equivalent to sampling the *H*-plane pattern in Fig. 3

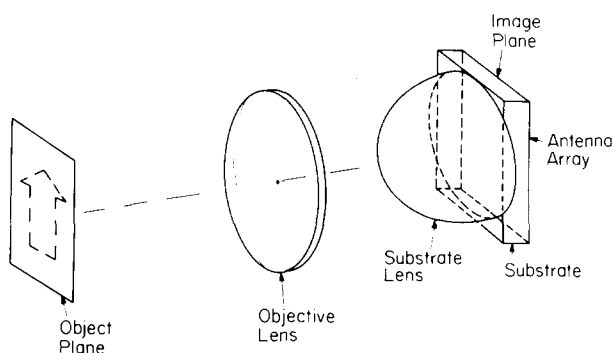


FIG. 1. "Reverse microscope" optical system for an imaging array.

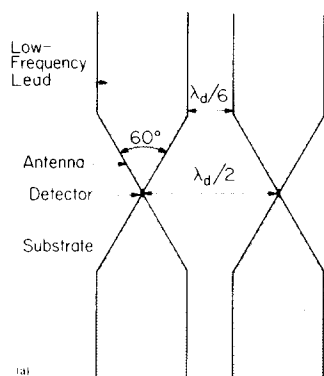


FIG. 2. (a) Bow-tie antenna array design and (b) photomicrograph of a single antenna showing how the microbolometer is formed where the bismuth strip crosses the gap between the arms of the bow. The microbolometer dimensions are $2 \times 5 \mu\text{m}$.

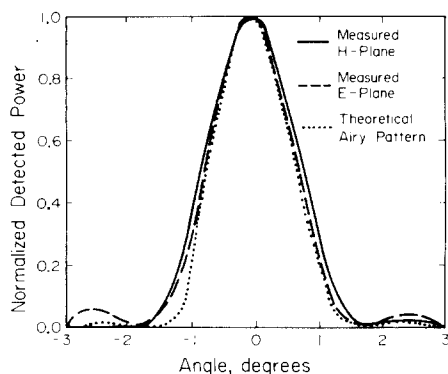
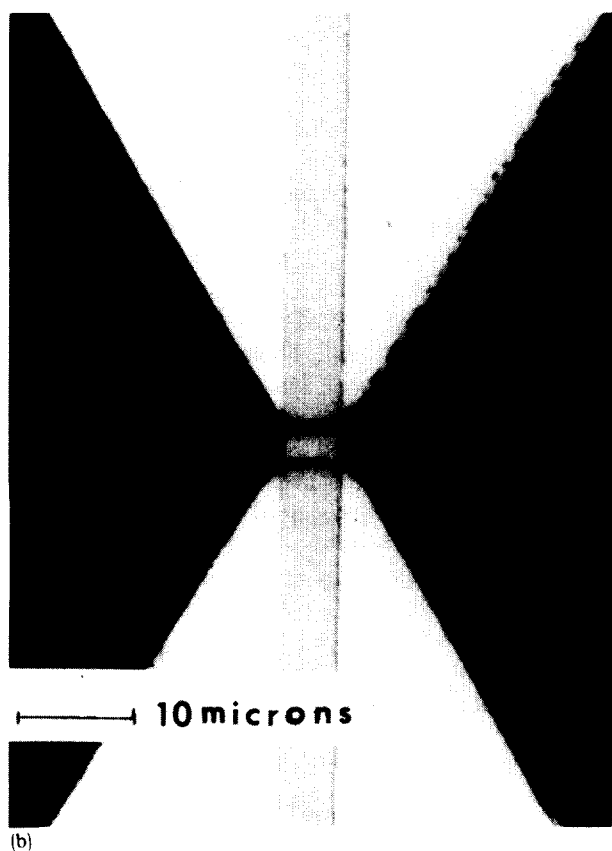


FIG. 3. System patterns at a single antenna. The *E*-plane pattern had another 12-dB sidelobe 5° off axis.

TABLE I. Normalized array point-source response.

Antenna	Response
Center	1
Nearest neighbor	0.40 ± 0.05
Next-nearest neighbor	0.01 ± 0.01

at intervals of 1.0° . This procedure was repeated three times on different groups of antennas. Table I summarizes the results. To the accuracy of the measurements the point-source response is symmetric. The calculated OTF for this point response is plotted in Fig. 4, along with the theoretical response of an ideal diffraction-limited system. The array response approaches the diffraction limit.

To demonstrate the resolution of the array we performed an experiment that is easier at millimeter wavelengths than at optical wavelengths: coherent illumination of two pinholes with varying relative phases. Our pinholes were 5-mm holes drilled in a copper plate, spaced to give a point-source separation 20% larger than the Rayleigh limit. Stacks of fused-quartz cover slips provided the phase delays. When the point sources are in quadrature, the intensity distribution is identical to that of two incoherent point sources (Ref. 14, p. 131). Figure 5 shows that the array resolves them easily. The remaining two images are for sources in phase and sources in phase opposition.

The measured responsivity of the array elements was $1-2 \text{ V/W}$ at the relatively low bias of 1 mA. Previous measurements¹⁵ have shown that the bolometers are $1/f$ noise limited up to 100 kHz and that they have a frequency response of 5 MHz. We expect the array to have a Johnson noise limited NEP from 100 kHz to 5 MHz of $10^{-9} \text{ W}/\sqrt{\text{Hz}}$. This sensitivity and speed should be adequate for far-infrared plasma interferometer measurements. Work is under way to determine the losses and coupling efficiencies. The field of view of the array, 8 antennas, is presently limited by the size of the substrate lens. We are now developing a system for a wavelength of $119 \mu\text{m}$.

In summary, we have demonstrated a far-infrared monolithic imaging antenna array with diffraction-limited

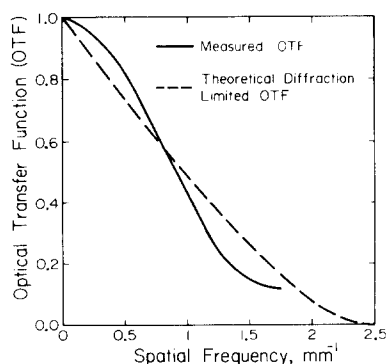


FIG. 4. Measured OTF compared with the theoretical diffraction-limited OTF (Ref. 14, p. 120). It is assumed that data processing will cut off the measured OTF at a spatial frequency of 1.75 mm^{-1} , the inverse of twice the antenna spacing.

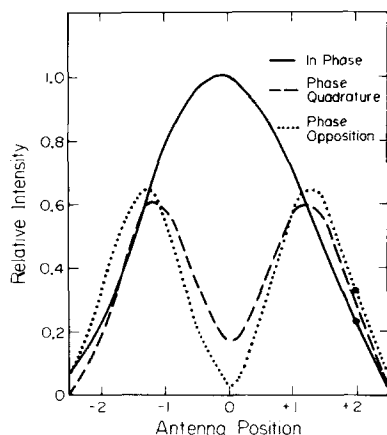


FIG. 5. Array images of two pinholes with varying relative phases. The points between the sampled antenna values were recovered by the standard sincfunction interpolation of sampling theory (Ref. 14 pp. 21–25). During the measurements, the bond on the antenna at +2 failed, and two data points were lost. To allow us to plot the entire curve, we filled in these two data points (solid circles) by symmetry.

resolution. The key innovations in the system are the “reverse-microscope” design that couples in radiation through a lens on the back of the substrate and the modified bow-tie antenna design.

We appreciate the support of the Jet Propulsion Laboratory and the Department of Energy under contract DE-AM03-765F-00010 Task IIA. We would like to thank Professor S. E. Schwarz at U. C. Berkeley for helping us with the mask making, Professor N. C. Luhmann, Jr., and Dr. W. A. Peebles at UCLA for the loan of evaporators and facilities,

and Professor O. Staffed at UCLA for suggesting that silver would be a better material for leads than gold.

- ¹J. P. Hollinger, J. E. Kenney, and B. E. Troy, Jr., *IEEE Trans. Microwave Theory Tech.* **MTT-24**, 786, (1977).
- ²D. T. Hodges, F. B. Foote, E. E. Reber, and R. L. Schellenbaum, *Conference Digest, 4th Int. Conf. on Infrared and Millimeter Waves and Their Applications*, IEEE Cat. No. 79 CH 1384-7 *MTT*, 1979, p. 51.
- ³J. Waldman, H. R. Fetterman, P. E. Duffy, T. G. Bryant, and P. E. Tannenwald, *4th Int. Conf. on Infrared and Millimeter Waves and Their Applications*, IEEE Cat. No. 79 CH 1384-7 *MTT*, 1979, p. 49.
- ⁴D. Veron, “Submillimeter Interferometry of High-Density Plasmas,” in *Infrared and Millimeter Waves*, edited by K. J. Button (Academic, New York, 1979), Vol. 2, p. 67.
- ⁵N. C. Luhmann, Jr., “Instrumentation and Techniques for Plasma Diagnostics: An Overview,” in *Infrared and Millimeter Waves*, edited by K. J. Button (Academic, New York, 1979), Vol. 2, p. 1.
- ⁶J. M. Schuchardt, J. M. Newton, T. P. Morton, and J. A. Gagliano, *Micro-wave J.* **45** (June, 1981).
- ⁷G. A. Gordon, R. L. Hartmann, and P. W. Kruse, “Imaging-Mode Operation of Active NMMW Systems,” *Infrared and Millimeter Waves*, edited by K. J. Button (Academic, New York, 1981), Vol. 4, p. 327.
- ⁸B. J. Clifton, R. A. Murphy, and G. D. Alley, *Conference Digest, 4th Int. Conf. on Infrared and Millimeter Waves and Their Applications*, IEEE Cat. No. 79 CH 1384-7 *MTT*, 1979, p. 84.
- ⁹B. J. Clifton, G. D. Alley, R. A. Murphy, and I. H. Mroczkowski, *IEEE Trans Electron Dev.* **ED-28**, 155 (1981).
- ¹⁰T. G. Phillips, D. P. Woody, G. J. Dolan, R. E. Miller, and R. A. Linke, *IEEE Trans. Magn.* **MAG-17**, 684 (1981).
- ¹¹T. L. Hwang, S. E. Schwarz, and D. B. Rutledge, *Appl. Phys. Lett.* **34**, 9 (1979).
- ¹²F. A. Jenkins and H. E. White, *Fundamentals of Optics*, 4th Ed. (McGraw-Hill, New York, 1975).
- ¹³D. B. Rutledge and M. S. Muha, *IEEE Trans. Ant. Propagat.* (to be published).
- ¹⁴J. W. Goodman, *Introduction to Fourier Optics* (McGraw-Hill, New York, 1968).
- ¹⁵D. B. Rutledge and S. E. Schwarz, *IEEE J. Quantum Electron.* **QE-17**, 407 (1981).

External off and on switching of a bistable optical device

S. S. Tarng, K. Tai, J. L. Jewell, and H. M. Gibbs
Optical Sciences Center, University of Arizona, Tucson, Arizona 85721

A. C. Gossard, S. L. McCall, A. Passner, T. N. C. Venkatesan, and W. Wiegmann
Bell Laboratories, Murray Hill, New Jersey 07974

(Received 28 September 1981; accepted for publication 17 November 1981)

A GaAs etalon has been switched on in a detector-limited time of 200 ps by a 10-ps, 600-nm, 1-nJ pulse and switched off in ≤ 20 ns by a 7-ns, 600-nm, 300-nJ pulse.

PACS numbers: 42.65.Gv, 71.35.+z, 85.60.Me

Optical bistable devices are being explored as basic components in all-optical signal processing and computing.^{1–3} Previously, intrinsic optical bistable devices have been switched on with external pulses.^{2,3} However, switch-off required a reduction of the input intensity below the switch-off intensity. For many applications it would be desirable to be able to switch the device in either direction with external pulses while maintaining the input intensity constant. Here is reported the first switch-off of an intrinsic optical bistable

device by an external pulse. It is a brute force technique in that enough energy is absorbed to heat the device thereby changing the characteristic curves so that the switch-off intensity is above the constant input intensity, resulting in excitonic switch-off. The mechanism is thus the same as for the self-switching of an unstable device undergoing regenerative pulsations.⁴ Although the present thermally actuated switch-off is unlikely to be practical it is a first step toward active switch-off.